Applied phenomics and genomics for improving barley yellow dwarf resistance in winter wheat

Paula Silva[1,2], Byron Evers[1], Alexandria Kieffaber[1], Xu Wang[3], Richard Brown[1], Liangliang Gao[1], Allan Fritz[4], Jared Crain[1], Jesse Poland[1,5,§]

[1] Department of Plant Pathology, College of Agriculture, Kansas State University, Manhattan, Kansas, 66506

[2] Programa Nacional de Cultivos de Secano, Instituto Nacional de Investigación Agropecuaria (INIA), Estación Experimental La Estanzuela, Colonia, Uruguay, 70006

[3] Department of Agricultural and Biological Engineering, University of Florida, IFAS Gulf Coast Research and Education Center, Wimauma, Florida, 33598

[4] Department of Agronomy, College of Agriculture, Kansas State University, Manhattan, Kansas, 66506

[5] King Abdullah University of Science and Technology, Thuwal, Saudi Arabia

[§] corresponding author: jpoland@ksu.edu, jesse.poland@kaust.edu.sa

ORCID

Paula Silva: 0000-0003-2655-2949

Byron Evers: 0000-0003-1840-5842

Xu Wang: 0000-0002-7144-6865

Liangliang Gao: 0000-0002-8562-0027

Allan Fritz: 0000-0003-2574-8675

Jared Crain: 0000-0001-9484-8325

Jesse Poland: 0000-0002-7856-1399

Running title – Phenomics and genomics for BYD

Keywords: Barley yellow dwarf (BYD), High-throughput Phenotyping (HTP), *Triticum aestivum*, Virus, Resistance, Tolerance, Genome-wide Association Mapping (GWAS), Genomic Selection (GS)

Abstract

Barley yellow dwarf (BYD) is one of the major viral diseases of cereals. Phenotyping BYD in wheat is extremely challenging due to similarities to other biotic and abiotic stresses. Breeding for resistance is additionally challenging as the wheat primary germplasm pool lacks genetic resistance, with most of the few resistance genes named to date originating from a wild relative species. The objectives of this study were to, i) evaluate the use of high-throughput phenotyping (HTP) from unmanned aerial systems to improve BYD assessment and selection, ii) identify genomic regions associated with BYD resistance, and iii) evaluate genomic prediction models ability to predict BYD resistance. Up to 107 wheat lines were phenotyped during each of five field seasons under both insecticide treated and untreated plots. Across all seasons, BYD severity was lower with the insecticide treatment and plant height (PTHTM) and grain yield (GY) showed increased values relative to untreated entries. Only 9.2% of the lines were positive for the presence of the translocated segment carrying resistance gene *Bdv2* on chromosome 7DL. Despite the low frequency, this region was identified through association mapping. Furthermore, we mapped a potentially novel genomic region for resistance on chromosome 5AS. Given the variable heritability of the trait (0.211 – 0.806), we obtained relatively good predictive ability for BYD severity ranging between 0.06 – 0.26. Including *Bdv2* on the predictive model had a large effect for predicting BYD but almost no effect for PTHTM and GY. This study was the first attempt to characterize BYD using field-HTP and apply GS to predict the disease severity. These methods have the potential to improve BYD characterization and identifying new sources of resistance will be crucial for delivering BYD resistant germplasm.

Introduction

Wheat (*Triticum aestivum* L.) is one of the most essential food crops in the world and is constantly threatened by several biotic stresses (Savary *et al.* 2019). Among the most important viral stresses is barley yellow dwarf (BYD). This disease is widespread across the world, caused by viruses and transmitted by aphids (Shah *et al*. 2012), and can cause significant yield reductions in susceptible cultivars. In Kansas, BYD is the fourth most significant wheat disease in terms of average estimated yield losses with an average yield loss of approximately 1% estimated over the past 20 years (Hollandbeck *et al*. 2019), equivalent to a loss of more than $10 million per year. However, yield losses are highly variable ranging from 5% to 80% in a single field depending on the environment, management practices, the host, and the genetic background, (Miller and Rasochová 1997; Perry *et al*. 2000; Gaunce and Bockus 2015). Moreover, the wide host range and the complex lifestyle of its vectors make BYD extremely difficult to manage, and different management strategies (e.g., planting date and control of vector populations) are inconsistent depending on climate and location (Bockus *et al*. 2016). Thus, in many production environments, particularly in the Central and Eastern regions of Kansas, BYD is often the most economically impactful disease.

Barley yellow dwarf disease symptoms are highly variable depending on the crop, variety, time, and developmental stage when the infection occurs, aphid pressure, and environmental conditions (Shah *et al*. 2012; Choudhury *et al*. 2019b). BYD characterization in the field is extremely challenging as the symptoms can easily be confused with other viral disease symptoms such as wheat streak mosaic virus symptoms, nutrient deficiencies, or environmental stresses like waterlogging (Shah *et al*. 2012). Typical BYD symptoms can be observed at all levels of plant organization – leaf, roots, and flowers. Leaf discoloration in shades of yellow, red, or purple, specifically starting at the tip of the leaf and spreading from the margins toward the base is common as well as a reduction in chlorophyll content (Jensen and Van Sambeek 1972; D'arcy 1995). Often the entire plant visually appears stunted or dwarfed from a reduction in biomass by reducing tiller numbers. Spike grain yield is decreased through a reduction in kernels per spike and kernel weight which also affects grain quality (Riedell *et al*. 2003; Choudhury *et al*. 2019b). Quality can be further reduced by a reduction in starch content (Peiris

et al. 2019). Below ground effects of BYD have also been reported including reduced root growth (Riedell *et al*. 2003).

Currently, there is no simple solution to control BYD (Walls *et al*. 2019), however, the use of genetic resistance and tolerance is the most appealing and cost-effective option to control this disease (Comeau and Haber 2002; Choudhury *et al*. 2017; 2019b). Resistance and tolerance could be different genetic mechanisms, namely stopping virus replication and minimizing disease symptoms respectively, but within this paper all mention of resistance includes both genetic resistance and tolerance. Breeding strategies involving genetic resistance can target either the aphids or the virus. Resistance to aphids can be achieved by three different strategies, antixenosis, antibiosis, or tolerance (Girvin *et al*. 2017). To date, most breeding efforts have been directed to the identification of viral tolerance, also known as 'field resistance', that refers to the ability of the plant to yield under BYD infection and is associated with a reduction of symptoms of infection independent of the virus titer (Foresman *et al*. 2016). Field resistance has been reported to be polygenic, falling under the quantitative resistance class, where several genes with very small effects control the resistance response (Qualset *et al*. 1973, Cisar *et al*. 1982; Ayala *et al*. 2002; Choudhury *et al*. 2019a; c).

Presently, no major gene conferring immunity or a strong resistant phenotype to BYD has been identified in bread wheat, and only four resistance genes have been described for BYD. Located on chromosome 7DS, *Bdv1* is the only gene described from the primary pool of wheat and was originally identified in the wheat cultivar 'Anza' (Qualset *et al*. 1984; Singh *et al*. 1993). This gene provides resistance to some but not all the viruses that cause BYD (Ayala-Navarrete and Larkin 2011). The other three named genes were all introduced into wheat through wide crossing from intermediate wheatgrass (*Thinopyrum intermedium*) (Ayala *et al*. 2001; Zhang *et al*. 2009). *Bdv2* and *Bdv3* are both located on a translocation segment on wheat chromosome 7DL (Brettell *et al*. 1988; Sharma *et al*. 1995), while *Bdv4* is located on a translocation segment on chromosome 2D (Larkin *et al*. 1995; Lin *et al*. 2007). *Bdv2* was the first gene successfully introgressed in wheat breeding programs from the tertiary gene pool for BYD resistance (Banks *et al*. 1995) and deployed into varieties.

In addition to the four known resistance genes, other genomic regions associated with BYD resistance have been identified through genetic mapping. These regions have been described on nearly all wheat chromosomes but have not been genetically characterized (Ayala *et al*. 2002; Jarošová *et al*. 2016; Choudhury *et al*. 2019a; b; c). Moreover, two recent studies have reported that some of these new genomic regions display additive effects (Choudhury *et al*. 2019a; b). Additive genetic effects had already been reported in lines combining *Bdv2* and *Bdv4* (Jahier *et al*. 2009).

Taken together, research indicates that resistance genes to BYD in wheat are rare. With a lack of major genes and difficulty to characterize resistance in the wheat pool likely due to the polygenic nature of many small effect loci, identifying resistance has been limited. Nevertheless, breeding programs have devoted large efforts for breeding BYD resistance due to the economic importance of this disease, with some of the greatest success coming from wide crosses to the tertiary gene pool.

Breeding for BYD resistance can be improved by applying strategies for more effective evaluation and utilization of the identified resistance. To get a better understanding of BYD and its quantitative nature, consistent and high-throughput methods are needed for the identification of resistant wheat lines for large-scale selection in breeding programs (Aradottir and Crespo-Herrera 2021). Effective selection on the quantitative resistance with low heritability can be aided by the high-throughput genotyping, high-throughput phenotyping (HTP), or a combination of both.

Access to high-density genetic markers at a very low-cost, owing to the rapid developments in DNA sequencing, have enabled breeding programs to apply molecular breeding for quantitative traits. Genomic selection (GS) is a powerful tool to breed for quantitative traits with complex genetic architecture and low heritability (e.g., yield, quality, and diseases such as Fusarium head blight), because it has greater power to capture loci with small effect compared with other marker-assisted selection strategies (Meuwissen *et al.* 2001; Poland and Rutkoski 2016). In addition to molecular data, HTP using unmanned aerial systems (UAS), or ground-based sensors is providing high density phenotypic data that can be incorporated into breeding programs to

increase genetic gain (Haghighattalab *et al*. 2016; Crain *et al.* 2018; Wang *et al.* 2020). Using precision phenotyping for disease scoring can improve the capacity for rapid and non-biased evaluation of large field-scale numbers of entries (Poland and Nelson 2011). Taken together improvements in genomics and phenomics have the potential to aid breeding progress for BYD resistance.

In an effort to accelerate the development of resistant lines, we combined high throughput genotyping and phenotyping to assess BYD severity in a large panel of elite wheat lines. We evaluated the potential of HTP data to accurately assess BYD severity as well as identify genetic regions associated with BYD resistance and inform whole genome prediction to identify resistant lines.

Materials and Methods

Plant Material

A total of 381 different wheat genotypes were characterized for BYD resistance, including 30 wheat cultivars and 351 advanced breeding lines in field nurseries over five years (Table S1). In each nursery, an unbalanced set of 52 – 107 wheat entries were evaluated including both cultivars and breeding lines (Table 1). The BYD susceptible cultivar 'Art' and BYD resistant cultivar 'Everest' were included in all the nurseries (seasons) as checks.

Field Experiments

Nurseries for BYD field-screening were conducted during five consecutive wheat seasons (2015 – 2016 to 2019 – 2020) (Table 1). Seasons 2015 – 16 and 2016 – 17 were conducted at Kansas State University (KSU) Rocky Ford experimental station (39˚13'45.60" N, 96˚34'41.21" W), while the 2017 – 18, 2018 – 19, and 2019 – 20 nurseries were planted at KSU Ashland Bottoms experimental station (39˚07'53.76" N, 96˚37'05.20" W). The nurseries were established for natural infections by planting about three weeks earlier than the normal planting window in mid-September. The susceptible cultivar 'Art' was planted as a spreader plot in the borders and as a control check plot also with the resistant cultivar 'Everest'. The experimental unit was 1.5m × 2.4m with a six-row plot on 20cm row spacing.

A split-plot field design with two or three replications was used where the main plot was insecticide treatment, and the split plot was the wheat genotype. Three replications were used for proof of concept during the first two seasons but then two replications were chosen as a balance of space and number of entries for the following seasons. For the treated replications the seed were treated at planting with Gaucho XT (combination of insecticide and fungicide) at a rate of 0.22 ml/100g of seed, followed with foliar insecticide applications starting from approximately 2 – 3 weeks after planting through heading. Depending on field conditions, spray treatments were conducted every 14 – 21 days if average air temperatures remained above 10°C. Foliar insecticides were applied to the treated replications in a spray volume of 280.5 L/ha using a Bowman MudMaster plot sprayer equipped with TeeJet Turbo TwinJet tips. Insecticide applications consisted of a rotation of Warrior II, Lorsban, and Mustang Max at rates of 0.14L/ha, 1.17L/ha, and 0.29L/ha, respectively. For the control insecticide treatment (untreated), the seed were treated with Raxil MD (fungicide) at a rate of 0.28ml/100g of seed, and no foliar insecticide applications were applied. Foliar fungicide Nexicor was applied to the whole experiment at a rate of 0.73L/ha, at both planting and heading, to control all other diseases so the main disease pressure was focused on BYD.

Phenotypic Data

Individual plots were assessed for i) BYD severity characterized as the typical visual symptoms of yellowing or purpling on leaves using a 0 – 100% visual scale, determined directly after spike emergence by recording the proportion of the plot exhibiting the symptoms (Table 1), ii) manual plant height ($PTHT_M$, meters), and iii) grain yield (GY, tons/ha). Experimental plots were harvested using a Kincaid 8XP plot combine (Kincaid Manufacturing., Haven, KS, USA). Grain weight, grain moisture and test weight measurements for each plot was recorded using a Harvest Master Classic GrainGage and Mirus harvest software (Juniper Systems, Logan, UT, USA). Visual phenotypic assessment was recorded using the Field Book phenoapp (Rife and Poland 2014).

206 **High-Throughput Phenotyping**

207 To compliment the manually recorded phenotypic data, we applied HTP using a ground-based
208 proximal sensing platform or an UAS (Table 2). Seasons 2015 – 16 and 2016 – 17 were
209 characterized by the ground platform as described in Barker *et al*. (2016) and Wang *et al*. (2018).
210 For the other three seasons, we used a quadcopter DJI Matrice 100 (DJI, Shenzhen, China)
211 carrying a MicaSense RedEdge-M multispectral camera (MicaSense Inc., United States). The
212 HTP data was collected on multiple dates throughout the growth cycle from stem elongation to
213 ripening (GS 30 – 90; Zadoks *et al*. 1974) (Table 2). Flight plans were created using CSIRO
214 mission planner application and missions were executed using the Litchi Mobile App (VC
215 Technology Ltd., UK, https://uavmissionplanner.netlify.app/) for DJI Matrice100. The aerial
216 image overlap rate between two geospatially adjacent images was set to 80% both sequentially
217 and laterally to ensure optimal orthomosaic photo stitching quality. All UAS flights were set at
218 20m above ground level at 2m/s and conducted within two hours of solar noon. To improve the
219 geospatial accuracy of orthomosaic images, white square tiles with a dimension of 0.30m ×
220 0.30m were used as ground control points and uniformly distributed in the field experiment
221 before image acquisition and surveyed to cm-level resolution using the Emlid REACH RS+
222 Real-Time Kinematic Global Navigation Satellite System unit (Emlid Ltd., HongKong, China).
223
224 An automated image processing pipeline (Wang *et al*. 2020) was used to generate the
225 orthomosaics and extract plot-level plant height ($PTHT_D$ (m), Singh *et al*. 2019) and the
226 normalized difference vegetation index (NDVI) (Rouse *et al*. 1974), calculated as:
227
228 $$NDVI = \frac{NIR-Red}{NIR+Red} \quad \text{[Eq. 1]}$$
229
230 where NIR and Red are the near-infrared and red bands of the multispectral images and NDVI is
231 the output image. Both traits were selected based on potential BYD characterization where the
232 most typical BYD symptoms include chlorosis and stunting of the plants, thus, influencing
233 NDVI and PTHT.

Statistical Data Analyses

First, the adjusted mean best linear unbiased estimator (BLUE) was calculated for each entry for all the different traits for each season (Table S1), using the following model:

$$y_{ijklm} = \mu + G_i + T_j + GT_{ij} + R_{k(j)} + B_{l(kj)} + C_{m(kj)} + e_{ijklm} \quad \text{[Eq. 2]}$$

where y_{ijklm} is the phenotype for the trait of interest, μ is the overall mean, G_i is the fixed effect of the i^{th} entry (genotype), T_j is the fixed effect of the j^{th} insecticide treatment, GT_{ij} is the fixed effect of the interaction between the i^{th} entry and the j^{th} insecticide treatment (genotype by treatment effect), $R_{k(j)}$ is the random effect of the k^{th} replication nested within the j^{th} insecticide treatment and distributed as iid $R_{k(j)} \sim N(0, \sigma_R^2)$, $B_{l(kj)}$ is the random effect of the l^{th} row nested within the k^{th} replication and j^{th} treatment distributed as iid $B_{l(kj)} \sim N(0, \sigma_B^2)$, $C_{m(kj)}$ is the random effect of the m^{th} column nested within the k^{th} replication and j^{th} treatment and assumed distributed as iid $C_{m(kj)} \sim N(0, \sigma_C^2)$, and e_{ijklm} is the residual for the $ijklm^{th}$ plot and distributed as iid $e_{ijklm} \sim N(0, \sigma_e^2)$. The 'lme4' R package (Bates *et al*. 2014) was used for fitting the models.

The BLUEs were used to inspect trait distributions and to calculate Pearson correlations between all traits. In addition, BLUE values were used to calculate the reduction in GY for each entry as the difference of GY between the untreated and insecticide treated main plots. This variable reflects the level of BYD resistance of each entry, and it was used to perform GWAS and GS analyses.

For NDVI and $PTHT_D$, the plot-level observed values extracted for the different phenotypic dates were fitted to a logistic non-linear regression model (Fox and Weisberg 2011) as,

$$y = \frac{\theta_1}{1 + e^{-(\theta_2 + \theta_3 x)}} + \varepsilon \quad \text{[Eq. 3]}$$

where is y the phenotype for the trait of interest at the time-point x measured as days after January 1, θ_1 is the maximum value (upper asymptote) represented by the final PTHT or maximum achieved NDVI, θ_2 is the inflection point that represents the greatest rate of change in the growth curve, either senescence for NDVI or height of growth, θ_3 is the lag phase or onset of senescence or growth rate from time x where x is the calendar day of the year since January 1, and ε is the residual error (Figure S1). The "nlme" R package was used for model fitting (Pinheiro *et al*. 2015). The model parameters obtained for each trait (θ_{1NDVI}, θ_{2NDVI}, θ_{3NDVI}, θ_{1PTHT_D}, θ_{2PTHT_D}, and θ_{3PTHT_D}) were used in addition to the other phenotypic traits to calculate BLUEs, distributions, correlations, and BLUPs.

Secondly, we used a mixed linear model to calculate the best linear unbiased predictors (BLUPs) for each entry in each nursery (season) (Table S1), using the same model as described in equation 2 but defining G_i, T_j, and GT_{ij} as random effects. BLUPs were used because of the unbalanced nature of the data (not all lines were evaluated in all the seasons). The BLUPs calculated for each season were then combined for GWAS and GS. Furthermore, we calculated broad-sense heritability on a line-mean basis by splitting the data based on whole plot treatment for insecticide treatments as:

$$H^2 = \frac{\sigma_G^2}{\sigma_G^2 + \frac{\sigma_e^2}{r}} \qquad \text{[Eq. 4]}$$

where σ_G^2 is the genotypic variance, σ_e^2 is the residual error variance, and r is the number of replications.

Genotypic Data

A total of 346 wheat entries were genotyped using genotyping-by-sequencing (GBS) (Poland *et al*. 2012) and sequenced on an Illumina Hi Seq2000. Single nucleotide polymorphisms (SNPs) were called using Tassel GBSv2 pipeline (Glaubitz *et al*. 2014) and anchored to the Chinese Spring genome assembly v1.0 (Appels *et al*. 2018). SNP markers with minor allele frequency < 0.01, missing data > 85%, or heterozygosity > 15% were removed from the analysis. After filtering, we retained 29,480 SNPs markers that were used to investigate the population structure

through principal component analysis (PCA), genome-wide association analysis (GWAS), and GS. In addition, GBS data was used to run a bioinformatics pipeline to predict the presence or absence of the translocated segment on chromomere 7DL carrying the *Bdv2* gene for each entry (Table S1). The prediction was done based on a modified alien predict pipeline (Gao *et al*. 2021). Briefly, alien or wheat specific tags were counted in the 7DL region and tabulated using a training set of cultivars or lines that are known to be *Bdv2* positive and negative. A simple classification was done based on alien to wheat tag counts ratios.

Genome-Wide Association Analysis

The GWAS analysis was performed with a mixed linear model implemented in the 'GAPIT' R package (Lipka *et al*. 2012) that includes principal components to account for population structure as fixed effects and the individuals to explains familial relatedness as random effects,

$$y = X\beta + Zu_i + e \qquad \text{[Eq. 5]}$$

where y is the vector of phenotypic BLUPs, X and Z are the incidence matrix of β and u_i, respectively, with u_i assumed ~ N $(0, 2K_i\sigma_i^2)$ where K is the individual kinship matrix, and e is the vector of random residual effects with ~ N $(0, \mathrm{I}\sigma_e^2)$, where I is the identity matrix and σ_e^2 is the unknown residual variance. The false discovery rate correction with an experimental significance level value of 0.01 was used to assess marker-trait associations. Manhattan plots were generated with 'CMplot' package in R software (Yin 2020). PCA using GBS-SNPs was performed in R language. Eigenvalues and eigenvectors were computed with 'e' function using 'A.mat' function and the 'mean' imputation method of 'rrBLUP' package (Endelman, 2011). To declare a quantitative trait locus (QTL) we considered only the regions having several SNP markers in linkage disequilibrium, clearly showing a peak. We did not consider regions with a single SNP above the significant threshold as a QTL.

Genomic Selection

Using data from the five seasons, GS models using the genomic best linear unbiased predictor (G-BLUP) were developed to assess predictive ability. A five-fold cross-validation method was used to assess model accuracy where the data set was split into five sets based on season, with

four seasons forming the training set and the fifth season serving as prediction set. This process was repeated until all seasons were predicted. Along with predicting all other seasons from each season, a model was evaluated with a leave-two-out cross-validation strategy. This strategy was used to get a better mix of years with and without disease incidence, where the training population consisted of three seasons, and the remaining two seasons were predicted from the combined training population. The GS model was fitted with the training population using 'rrBLUP' *kin.blup* function (Endelman 2011), the GS model equation was,

$$y = Wg + \varepsilon \qquad \text{[Eq. 6]}$$

where y is a vector of phenotypic BLUPs, W is the design matrix of g, g is the vector of genotypic values ~ N $(0, K\sigma_g^2)$ and ε is the vector of residual errors (Endelman 2011). Predictive ability was assessed using Pearson's correlation (r) between the predicted value (G-BLUP) and the BLUP for the respective phenotype. In addition, for both GS strategies we also tested the effect of adding the genotype of the *Bdv2* loci as a fixed effect cofactor, using the model,

$$y = \mu + \boldsymbol{X}\beta + \boldsymbol{W}g + \varepsilon \qquad \text{[Eq. 7]}$$

which combines parameters described in equation 6 and X is the matrix $(n\ x\ 1)$ of individual observation for presence or absence of *Bdv2* and β is the fixed effect for the *Bdv2* measurements.

Results

Phenotypic Data

We analyzed five years of BYD field-screening nurseries (seasons 2015-16 to 2019-20) characterizing a total of 381 wheat lines. The disease pressure and the expression of BYD associated symptoms varied each season, however, we were able to observe a significant effect of the insecticide treatment in all seasons (Figure 1). Across all seasons, BYD symptoms were lower on the insecticide treated plots and both $PTHT_M$ and GY increased compared to the non-treated control. Season 2016-17 had the most conducive conditions for BYD screening, resulting

in high average severity and a larger difference between mean values for the treated vs untreated plots for all the collected traits (Figure 1). There was general consistency in order across all seasons with the susceptible check 'Art' ranked among the highest in BYD severity (Figure S2).

Phenotypic correlations between the traits showed a negative correlation between BYD and GY for all the seasons and a negative or no correlation between BYD and $PTHT_M$ (Figure S3). The same correlation trends were observed under insecticide treated and untreated plots. Broad-sense heritability was moderate to high for all the traits, ranging between 0.21 and 0.79 for the insecticide treated plots and between 0.41 and 0.84 for the untreated plots. Across all traits, the untreated insecticide replications showed higher H^2values, with season 2016 – 17 showing the highest values (Figure 2).

For the HTP data collected (Table 2), we obtained three different parameters (θ_1, θ_2, and θ_3) for both $PTHT_D$ and NDVI after fitting a logistic regression model using the data collected during the experiments (2015-16 season data was not included due to lack of data quality) (Figure S1). Correlations between these parameters and the phenotypic traits collected manually were different for all the traits (Figure S3). For the insecticide untreated plots, BYD resulted in a negative correlation with θ_{2NDVI} and a positive correlation with θ_{3NDVI}, in most of the field seasons. We did not find a clear correlation pattern between BYD and $PTHT_D$. For $PTHT_M$ we detected a positive correlation with θ_{1PTHT_D}across all seasons, and for GY we observed a positive correlation with θ_{1NDVI} and θ_{2NDVI}, and a negative correlation with θ_{3NDVI} (Figure S3).

Prediction of *Bdv2* Resistance Gene

We used GBS data to genotype the *Bdv2* resistance gene located on a translocation segment from intermediate wheatgrass on chromosome 7DL of bread wheat. In total, 33 of the 346 wheat lines carried the *Th. intermedium* chromosomal translocation with *Bdv2* (Table S1). Interestingly, 28 of these *Bdv2* lines belonged to the same breeding cycle, entering the advanced yield nursery stage of the KSU breeding program in the 2017 – 18 season. Furthermore, only 7 pedigrees are represented within the 28 *Bdv2* entries, meaning that these lines are highly related. The remaining 5 *Bdv2* lines were distributed in 2015 – 16 (n=3), 2018 – 19 (n=1), and 2019 – 20 (n=1), and none of the lines from the season 2016 – 17 had the presence of *Bdv2* (Table S1).

386

387 **Population Structure**

388 We studied the population structure of 346 wheat lines using 29,480 GBS-derived SNP markers.
389 The PCA did not reveal a strong pattern of population structure (Figure 3). Moreover, the
390 variation explained by the first two principal components (4 and 3%, respectively) also supports
391 the hypothesis of minimal population structure within a single breeding program. We observed
392 that most of the wheat cultivars released by KSU breeding program were located outside the
393 cluster grouping all the breeding lines (Figure 3A). Lines with the presence of *Bdv2* clustered
394 together (Figure 3B), likely due to a related pedigree to the original source, and we did not
395 identify any evident pattern for BYD severity associated with the population structure (Figure
396 3C).

397

398 **Genome-Wide Association Analysis**

399 To investigate the genetic architecture of BYD we performed GWAS analyses for all collected
400 traits using the BLUP values for 346 lines and 29,480 SNP markers. The first two principal
401 components from PCA and the kinship matrix were included in the mixed model to account for
402 population structure and genetic relatedness. We found significant marker-trait associations for
403 BYD severity on chromosomes 5AS, 7AL, and 7DL (Figure 4A). The highest peak was
404 observed on the proximal end of chromosome 7DL, located at 571 Mbp – 637 Mbp. To test the
405 hypothesis that this association was explained by the resistance gene *Bdv2* (located on
406 chromosome 7DL), we investigated the haplotypes defined by the 16 SNP markers associated
407 with BYD severity and were able to identify two haplotypes that exactly matched the presence or
408 absence of *Bdv2* (Fig 4A). This same region was mapped using BYD severity and the presence
409 or absence of *Bdv2* as a fixed covariate (Figure 4B). This analysis (Figure 4B) also detected a
410 peak on chromosome 7AL. Lastly, we explored the effect of *Bdv2* on both BYD BLUEs and
411 BLUPs, and we observed that the presence of *Bdv2* had a positive effect in reducing the disease
412 severity by approximantly 10% (Figure 5A). The significant peak on chromosome 5AS, located
413 at 46 Mbp – 103 Mbp, was explained by 10 SNP markers, comprising two main haplotypes, one
414 of them associated with reduced BYD severity (Fig 5B). When we combined the different 5AS
415 haplotypes with *Bdv2*, we observed that the presence of *Bdv2* had a positive effect, reducing the
416 levels of BYD when combined with both 5AS haplotypes (Figure 5C), and suggesting an

417 additive effect. Compared to the associations found for *Bdv2* (Fig 4B), we did not find any
418 strong evidence of marker trait associations for the other evaluated traits (Figure S4).
419
420 **Genomic Selection**
421 To evaluate the potential of GS to predict BYD disease severity, we fit several GS models to the
422 phenotypic BLUPs of BYD, PTH_M, and reduction in GY. Across all traits, to determine
423 predictive ability we used a five-fold cross validation where prediction ability ranged from -0.08-
424 0.26. There was relatively good predictive ability for BYD severity ranging between 0.06 –
425 0.26, in comparison with $PTHT_M$ and reduction in GY resulting in a lower range from 0.02 – 017
426 and -0.08 – 0.2, respectively (Figure 6). Evaluating the conformation of the training population,
427 we observed that when including 2016-17 season, prediction abilities were the highest for BYD
428 but the lowest for the other two traits, implying that season 2016 – 17 was either a good season
429 to train the prediction models or a difficult season to predict based on available data.
430
431 To further investigate the power of GS, we developed models using a leave-two-out strategy,
432 where two seasons were excluded from the training population and used as the testing
433 population. We fitted GS models for all possible two-season combinations. This strategy
434 resulted in slightly smaller training populations which decreased overall predictive ability
435 (Figure 6). This result was evident for BYD predictions were excluding two seasons had a larger
436 negative impact.
437
438 Lastly, we evaluated the effect of adding information about the genotype of the *Bdv2* resistance
439 gene as a phenotypic fixed covariate into the GS models. There were differences in the effect of
440 *Bdv2* on the predictive ability across BYD severity, $PTHT_M$, and GY, showing a large effect for
441 predicting BYD but almost no effect for $PTHT_M$ and reduction in GY (Figure 6). The improved
442 predictive ability for BYD was clearly reflected with the decrease of prediction ability obtained
443 when season 2017 – 18 was excluded from the training population since most of the lines with
444 the presence of *Bdv2* were evaluated in that season.
445

Discussion

Phenotypic Data

The success of breeding for BYD resistance is highly impacted by the ability to precisely characterize breeding material and disease symptoms. Even though BYD is spread worldwide, its incidence in a given year depends on several factors such as aphid pressure, planting date, and environmental conditions (e.g., temperature, rainfall, frost, etc.). In this study, we evaluated winter wheat advanced breeding lines during five seasons implementing a rigorous field-testing approach, that ultimately enabled us to consistently have plots contrasting with BYD infection and uninfected or low incident plots. Moreover, by using large yield-size plots we were able to calculate the reduction in GY and use this parameter as an estimate of field resistance.

The expression of BYD symptoms, however, was highly inconsistent during the different seasons. Seasons 2015-16 and 2016-17 showed the best expression of the disease symptoms, supported by the wide range of BYD severity between treated and untreated replications (Figure 1). Interestingly, both these seasons were conducted in the same experimental field (Table 1), suggesting that this location could favor the expression of BYD. Moreover, weather conditions were variable for all the seasons, suggesting that these had a huge impact on the disease occurrence. While temperature records were similar for all the seasons, precipitation records did show some differences. Season 2017 – 18 was dryer than normal, with 34% less precipitation than the 30 years historical average (1981 – 2010). On the other hand, season 2018-19 was wetter than normal, with 58% more precipitation than the 30 years historical average (Table S2).

High-Throughput Phenotyping

Evaluating BYD resistance using visual phenotypic selection can be challenging due to the complex nature of the disease and rater variability (Poland and Nelson 2011). The use of HTP with UAS is gaining popularity within breeding programs because it further improves selection based on classical phenotyping. Accurate phenotyping is crucial for understanding the genetic basis of quantitative and complex traits like BYD. In this study, we used HTP to complement the visual BYD scoring. This tool improved our capacity for rapid, non-destructive, and non-biased evaluation of large field-scale numbers of entries for BYD resistance. We were able to

477 determine strong correlation patterns between visual BYD severity and HTP derived parameters
478 (Figure S3). However, none of the traits collected with UAS had a common genetic base with
479 BYD severity (Figure 4 and Figure S4). Disease scoring using HTP is scaling fast among
480 breeding programs; however, how to effectively use this data remains challenging. Some studies
481 have shown that data collected with sensor-based tools can be substituted to improve classical
482 disease visual evaluation (Sankaran *et al*. 2010; Kumar *et al*. 2016; Zheng *et al*. 2018); however,
483 to the best of our knowledge this study is the first attempt to characterize BYD in wheat using
484 HTP.
485
486 **Genome-Wide Association Analysis**
487 Using GWAS we detected QTLs on chromosomes 5AS, 7AL, and 7DL for BYD severity BLUPs
488 values. Using GBS tags that mapped to known alien fragments, we confirmed *Bdv2* resistance
489 gene was located at 7DL, and confirmed that the 7DL QTL was explained by the presence of the
490 *Bdv2* resistance gene. Even though only 33 wheat lines were positive for the presence of *Bdv2*,
491 we still had enough power to detect its effect, suggesting that *Bdv2* has a strong effect on BYD
492 under Kansas field conditions (Figure 5). The associations on chromosome 7AL, observed for
493 both BYD severity and *Bdv2*, suggest that the SNP markers on the 7AL peak may be miss-
494 anchored markers that should have mapped to 7DL. The relatively high heritability values
495 obtained for the untreated replications (Figure 2) allowed us to detect a minor QTL on 5AS.
496 Marza *et al*. (2005) reported a QTL at 38cM on the short arm of chromosome 5A associated with
497 yellowing symptoms caused by BYD, and it is possible that this is the same region yet more data
498 is needed to confirm if these QTLs are the same. The only other study reporting GWAS for BYD
499 in wheat was able to identify several markers associated with BYD resistance on chromosomes
500 2A, 2B, 6A, and 7A (Choudhury *et al*. 2019b). However, most of the association were explained
501 by individual SNP markers, and to date do not have any definitive biological link. GWAS
502 results for the other traits used in this study did not discover genomic regions associated with the
503 traits (Figure S4). Taken together, these results suggest that BYD resistance is not controlled by
504 any large effect loci that could easily be incorporated into the breeding program, thus GS could
505 be an efficient way to enhance BYD resistance.
506

Genomic Selection

We evaluated several different GS models to identify the best approach for predicting BYD (Figure 6). Overall, we observed some trends including i) incorporating years with consistent BYD disease data in the training population increased the model predictive ability, ii) predicting years with high disease pressure is difficult, iii) using major effect QTL, such as *Bdv2*, had increased prediction performance, suggesting that it is responsible for much of the predictive power. These results suggest that GS based on G-BLUP with *Bdv2* as fixed effects would lead to the greatest genetic gain for BYD breeding. Using selected major QTL as a fixed effect to improve GS models was suggested in a simulation study (Bernardo 2014) and demonstrated with empirical studies (Rutkoski *et al*. 2014). Nonetheless, using *Bdv2* as a fixed effect in our GS strategies did not consistently improve the predictive ability for PTH_M or reduction in GY (Rice and Lipka 2019). However, there was not a consistent distribution of *Bdv2* allele across the cohorts. BYD predictions were low compared to other disease (reviewed by Poland and Rutkoski 2016). However, since this is the first report of GS for BYD resistance in wheat, we do not have similar results to make better comparisons. BYD has traditionally been reported to have low H^2 (Tola and Kronstad 1984; Choudhury *et al*., 2019b) and in this study, even with well managemed plots that often had H^2 approaching 0.8, we still had difficulty reproducing these results year to year as evidence of the challenge of studying this pathosystem. Moreover, the correlation between HTP parameters and BYD phenotypes was interesting, but not sufficient to be useful in combination with GS in the germplasm tested.

Conclusions

We were able to show that *Bdv2* has a major effect controlling BYD resistance in the KSU breeding germplasm. Apart from the known *Bdv2* and a potentially novel 5AS region, we did not find evidence of other regions controlling BYD resistance supporting the hypothesis of limited resistance available in the current wheat gene pool and the highly polygenic nature of the trait. Moreover, our study was the first attempt to characterize and improve BYD field-phenotyping using HTP and apply GS to predict the disease. HTP traits showed strong correlation patterns with BYD severity, however, none of these parameters shared a common genetic architecture with BYD severity. The GS predictive ability results that we found in this study open the door for further improvement and testing GS implementation for breeding for

538 BYD resistance. Continuing the improvement of BYD characterization and the search of new
539 sources of resistance using species related to wheat, will be crucial to broadening the resistant
540 genes available to introgress into wheat germplasm.
541
542
543 **Data Availability Statement**
544 Supplemental material, including raw and analyzed phenotypic data, genotypic data,
545 supplementary tables and figures, and basic plot scripts are available at Dyrad
546 doi:10.5061/dryad.ncjsxkswd (temporary link: https://datadryad.org/stash/share/xkKdr62QYB-
547 YA93mkzq18_4yFUgwdnvv0uZUyuEHpAI) and GitHub
548 https://github.com/umngao/wsm1_bdv2
549 **Supplementary data description**
550 **Table S1 –** List of wheat entries phenotypically evaluated in the study. The table includes the
551 type of entry (cultivar or breeding line), the season that the entry was evaluated, the result for the
552 prediction of the presence/absence of the segment carrying the resistance gene *Bdv2*, and the best
553 linear unbiased predictors (BLUPs) for all the phenotypic traits collected.
554 **Table S2 –** Precipitation (inches) during the five field seasons in Riley County, KS, where
555 Rocky Ford and Ashland Bottoms experimental units are located. Normal temperature is defined
556 as a 30–year average from 1981 – 2010. Data was obtained from Kansas State University
557 (http://climate.k-state.edu/precip/county/)
558 **Figure S1 –** Growth trajectories and adjustment of the non-linear regression model of wheat
559 lines for A-B) normalized difference vegetation index (NDVI) and C-D) digital plant height
560 (meters). The data used correspond to season 2016 – 17 phenotypic data. Calendar days is the
561 number of days starting at January 1, 2017.
562 **Figure S2 –** Boxplots showing the phenotypic response of the wheat checks 'Art' (susceptible)
563 and 'Everest' (tolerant) for A) barley yellow dwarf (BYD) disease severity (%), B) manual plant
564 height ($PTHT_M$) (m) and C) grain yield (GY) (tons/ha). Adjusted phenotypic values are shown
565 for both insecticide treatment replications (treated and untreated).
566 **Figure S3 –** Scatterplots showing distribution and Pearson's correlation values for the
567 phenotypic traits studied during all the field seasons under two insecticide treatments (treated

568 and untreated). A-B) season 2016 – 17, C-D) season 2017 – 18, E-F) season 2018 – 19, and G-H)
569 season 2019 – 20.
570 **Figure S4 –** Manhattan plots showing genome-wide association analysis (GWAS) results for the
571 phenotypic traits collected during the study.
572
573 **Acknowledgements**
574 This material is based upon work supported by Kansas Wheat Commission Award No: B65336
575 "Integrative and Innovative Approaches to Diminish Barley Yellow Dwarf Epidemics Kansas
576 Wheat". PS was supported through a U.S. Fulbright-ANII Uruguay Scholarship. Any opinions,
577 findings, and conclusions or recommendations expressed in this material are those of the
578 author(s) and do not necessarily reflect the views of industry partners.
579
580

Literature Cited

Appels, R., K. Eversole, C. Feuillet, B. Keller, J, Rogers, *et al*., 2018 Shifting the limits in wheat research and breeding using a fully annotated reference genome. Science, 361(6403) http://dx.doi. org/10.1126/ science.aar7191

Aradottir, G. I., and L. Crespo-Herrera, 2021 Host plant resistance in wheat to barley yellow dwarf viruses and their aphid vectors: a review. Current Opinion in Insect Science, 2021, 45:59–68 https://doi.org/10.1016/j.cois.2021.01.002

Ayala-Navarrete, L., and P. Larkin, 2011 Wheat virus diseases: breeding for resistance and tolerance. World wheat book: a history of wheat breeding, Lavoisier, Paris, 2, 1073-107.

Ayala, L., M. Henry, M. Van Ginkel, R. Singh, B. Keller, *et al*., 2002 Identification of QTLs for BYDV tolerance in bread wheat. Euphytica, 128(2), 249-259 https://doi.org/10.1023/A:1020883414410

Ayala, L., M. Van Ginkel, M. Khairallah, B. Keller, and M. Henry, 2001 Expression of *Thinopyrum intermedium*-derived Barley yellow dwarf virus resistance in elite bread wheat backgrounds. Phytopathology, 91(1), 55–62 https://doi.org/10.1094/PHYTO.2001.91.1.55

Banks, P. M., J. L. Davidson, H. Bariana, and P. J. Larkin, 1995 Effects of barley yellow dwarf virus on the yield of winter wheat. Australian Journal of Agricultural Research, 46(5), 935-946

Barker III, J., N. Zhang, J. Sharon, R. Steeves, X. Wang, *et al*., 2016 Development of a field-based high-throughput mobile phenotyping platform. Computers and Electronics in Agriculture, 122, 74-85 https://doi.org/10.1016/j.compag.2016.01.017

Bates, D., M. Mächler, B. Bolker, and S. Walker, 2014 Fitting linear mixed-effects models using lme4. arXiv preprint arXiv:1406.5823

Bernardo, R., 2014 Genome-wide selection when major genes are known. Crop Science, 54(1), 68-75 https://doi.org/10.2135/cropsci2013.05.0315

Bockus, W. W., E. D. De Wolf, and T. Todd, 2016 Management strategies for barley yellow dwarf on winter wheat in Kansas. Plant Health Progress, 17(2), 122–127 https://doi.org/10.1094/PHP-RS-15-0050

610 Brettell, R. I. S., P. M. Banks, Y. Cauderon, X. Chen, z. Cheng, *et al*., 1988 A single wheatgrass
611 chromosome reduces the concentration of barley yellow dwarf virus in wheat. Annals of
612 Applied Biology, 113(3), 599–603 https://doi.org/10.1111/j.1744-7348.1988.tb03337.x
613 Choudhury, S., H. Hu, Y. Fan, P. Larkin, M. Hayden, *et al*., 2019a Identification of new QTL
614 contributing to barley yellow dwarf virus-PAV (BYDV-PAV) resistance in wheat. Plant
615 Disease, 103(11), 2798–2803 https://doi.org/10.1094/PDIS-02-19-0271-RE
616 Choudhury, S., P. Larkin, H. Meinke, M. D. Hasanuzzaman, P. Johnson, and M. Zhou, 2019b
617 Barley yellow dwarf virus infection affects physiology, morphology, grain yield and flour
618 pasting properties of wheat. Crop and Pasture Science, 70(1), 16-25
619 https://doi.org/10.1071/CP1836
620 Choudhury, S., P. Larkin, R. Xu, M. Hayden, K. Forrest, *et al*., 2019c Genome wide association
621 study reveals novel QTL for barley yellow dwarf virus resistance in wheat. BMC
622 genomics, 20(1), 1-8 https://doi.org/10.1186/s12864-019-6249-1
623 Choudhury, S., H. Hu, H. Meinke, S. Shabala, G. Westmore, *et al*., 2017 Barley yellow dwarf
624 viruses: infection mechanisms and breeding strategies. Euphytica, Vol. 213, pp. 1–22
625 https://doi.org/10.1007/s10681-017-1955-8
626 Cisar, G., C. M. Brown, and H. Jedlinski, 1982 Diallel analyses for tolerance in winter wheat to
627 the barley yellow dwarf virus 1. Crop Science, 22(2), 328-333
628 Comeau, A., and S. Haber, 2002 Breeding for BYDV tolerance in wheat as a basis for a multiple
629 stress tolerance strategy. Barley Yellow Dwarf Disease: Recent Advances and Future
630 Strategies, 82
631 Crain, J., S. Mondal, J. Rutkoski, R. P. Singh, and J. Poland, 2018 Combining High-Throughput
632 Phenotyping and Genomic Information to Increase Prediction and Selection Accuracy in
633 Wheat Breeding. The Plant Genome, 11(1), 170043
634 https://doi.org/10.3835/plantgenome2017.05.0043
635 D'arcy, C. J., 1995 Symptomatology and host range of barley yellow dwarf. Barley yellow
636 dwarf, 40, 9-28
637 Endelman, J. B., 2011 Ridge Regression and Other Kernels for Genomic Selection with R
638 Package rrBLUP. The Plant Genome, 4(3), 250–255.
639 https://doi.org/10.3835/plantgenome2011.08.0024

Foresman, B. J., R. E. Oliver, E. W. Jackson, S. Chao, M. P. Arruda, *et al*., 2016 Genome-wide association mapping of barley yellow dwarf virus tolerance in spring oat (*Avena sativa* L.). PloS one, 11(5), e0155376 https://doi.org/10.1371/journal.pone.0155376

Fox, J., and S. Weisberg, 2011 Nonlinear regression and nonlinear least squares in R. In: J. Fox and S. Weisberg, An R companion to applied regression. 2nd ed. SAGE Publications, Los Angeles, CA

Gao, L., D. H. Koo, P. Juliana, T. Rife, D. Singh, *et al*., 2021 The *Aegilops ventricosa* $2N^v$ S segment in bread wheat: cytology, genomics, and breeding. Theoretical and Applied Genetics, 134(2), 529-542. https://doi.org/10.1007/s00122-020-03712-y

Gaunce, G. M., and W. W. Bockus, 2015 Estimating Yield Losses Due to Barley Yellow Dwarf on Winter Wheat in Kansas Using Disease Phenotypic Data. Plant Health Progress, 16(1), 1–6 https://doi.org/10.1094/php-rs-14-0039

Girvin, J., R. J. Whitworth, L. M. A. Rojas, and C. M. Smith, 2017 Resistance of select winter wheat (*Triticum aestivum*) cultivars to *Rhopalosiphum padi* (Hemiptera: *Aphididae*). Journal of Economic Entomology, 110(4), 1886–1889 https://doi.org/10.1093/jee/tox164

Glaubitz, J. C., T. M. Casstevens, F. Lu, J. Harriman, R. Elshire, *et al*., 2014 TASSEL-GBS: A High-Capacity Genotyping by Sequencing Analysis Pipeline. PLoS ONE, 9(2), e90346 https://doi.org/10.1371/journal.pone.0090346

Haghighattalab, A., L. G. Pérez, S. Mondal, D. Singh, D. Schinstock, *et al*., 2016 Application of unmanned aerial systems for high throughput phenotyping of large wheat breeding nurseries. Plant Methods, 12(1), 1–15 https://doi.org/10.1186/s13007-016-0134-6

Hollandbeck, G. F., E. DeWolf, and T. Todd, 2019 Kansas cooperative plant disease survey report. Preliminary 2019 Kansas wheat disease loss estimates. October 2, 2019 https://agriculture.ks.gov/divisionsprograms/plant-protect-weed-control/reports-and-publications

Jahier, J., F. Chain, D. Barloy, A. M. Tanguy, J. Lemoine J, *et al*., 2009 Effect of combining two genes for partial resistance to Barley yellow dwarf virus-PAV (BYDV- PAV) derived from *Thinopyrum intermedium* in wheat. Plant Pathol 2009, 58:807-814 https://doi.org/10.1111/j.1365-3059.2009.02084.x

669 Jarošová, J., E. Beoni, and J. K. Kundu, 2016 Barley yellow dwarf virus resistance in cereals:
670 Approaches, strategies, and prospects. Field Crops Research, 198, 200–214
671 https://doi.org/10.1016/j.fcr.2016.08.030
672 Jensen, S. G., and J. W. Van Sambeek, 1972 Differential Effects of Barley Yellow Dwarf Virus
673 on the Physiology of Tissues of Hard Red Spring Wheat. Phytopathology, 62(2), 290
674 https://doi.org/10.1094/phyto-62-290
675 Kumar, S., M. S. Röder, R. P. Singh, S. Kumar, R. Chand, *et al*., 2016 Mapping of spot blotch
676 disease resistance using NDVI as a substitute to visual observation in wheat (*Triticum*
677 *aestivum* L.). Molecular Breeding, 36(7), 1–11 https://doi.org/10.1007/s11032-016-0515-
678 6
679 Larkin, P. J., P. M. Banks, E. S. Lagudah, R. Appels, C. Xiao, *et al*., 1995 Disomic *Thinopyrum*
680 *intermedium* addition lines in wheat with barley yellow dwarf virus resistance and with
681 rust resistances. Genome, 38(2), 385–394 https://doi.org/10.1139/g95-050
682 Lin, Z. S., Z. F. Cui, X. Y. Zeng, Y. Z. Ma, Z. Y. Zhang, *et al*., 2007 Analysis of wheat-
683 *Thinopyrum intermedium* derivatives with BYDV-resistance: Analysis of wheat-
684 *Th.intermedium* derivatives. Euphytica, 158(1–2), 109–118
685 https://doi.org/10.1007/s10681-007-9435-1
686 Lipka, A. E., F. Tian, Q. Wang, J. Peiffer, M. Li, *et al*., 2012 GAPIT: genome association and
687 prediction integrated tool. Bioinformatics, 28(18), 2397–2399
688 https://doi.org/10.1093/bioinformatics/bts444
689 Marza, F., G. H. Bai, B. F. Carver, and W. C. Zhou, 2005 Quantitative trait loci for yield and
690 related traits in the wheat population Ning7840× Clark. Theoretical and Applied
691 Genetics, 112(4), 688-698 https://doi.org/10.1007/s00122-005-0172-3
692 Meuwissen, T. H., B. J. Hayes, and M. E. Goddard, 2001 Prediction of total genetic value using
693 genome-wide dense marker maps. Genetics, 157(4), 1819-1829
694 https://doi.org/10.1093/genetics/157.4.1819
695 Miller, W. A., and L. Rasochová, 1997 Barley yellow dwarf viruses. Annual Review of
696 Phytopathology, Vol. 35, pp. 167–190 https://doi.org/10.1146/annurev.phyto.35.1.167
697 Mondal, S., J. E. Rutkoski, G. Velu, P. K. Singh, L. A. Crespo-Herrera, *et al*., 2016 Harnessing
698 diversity in wheat to enhance grain yield, climate resilience, disease and insect pest

699 resistance and nutrition through conventional and modern breeding approaches. Frontiers
700 in plant science, 7, 991 https://doi.org/10.3389/fpls.2016.00991
701 Perry, K. L., F. L. Kolb, B. Sammons, C. Lawson, G. Cisar, *et al*., 2000 Yield effects of Barley
702 yellow dwarf virus in soft red winter wheat. Phytopathology, 90(9), 1043–1048
703 https://doi.org/10.1094/PHYTO.2000.90.9.1043
704 Peiris, K. H., R. L. Bowden, T. C. Todd, W. W. Bockus, M. A. Davis, *et al*., 2019 Effects of
705 barley yellow dwarf disease on wheat grain quality traits. Cereal Chemistry, 96(4), 754-
706 764 https://doi.org/10.1002/cche.10177
707 Pinheiro, J., D. Bates, S. DebRoy, and D. Sarkar, 2015 R Core Team. 2015. *nlme*: linear
708 and nonlinear mixed effects models. R package version 3.1-120. R package version, 3-1.
709 Poland, J., 2015 Breeding-assisted genomics. Current Opinion in Plant Biology, Vol. 24, pp.
710 119–124 https://doi.org/10.1016/j.pbi.2015.02.009
711 Poland, J. A., and R. J. Nelson, 2011 In the eye of the beholder: The effect of rater variability
712 and different rating scales on QTL mapping. Phytopathology, 101(2), 290–298
713 https://doi.org/10.1094/PHYTO-03-10-0087
714 Poland, J. A., P. J. Brown, M. E. Sorrells, and J. L. Jannink, 2012 Development of high-density
715 genetic maps for barley and wheat using a novel two-enzyme genotyping-by-sequencing
716 approach. PloS one, 7(2), e32253 https://doi.org/10.1371/journal.pone.0032253
717 Poland, J., and J. Rutkoski, 2016 Advances and Challenges in Genomic Selection for Disease
718 Resistance. Annual Review of Phytopathology, 54(1), 79–98
719 https://doi.org/10.1146/annurev-phyto-080615-100056
720 Qualset, C. O., J. C. Williams, M. A. Topcu, and H. E. Vogt, 1973 The barley yellow-dwarf
721 virus in wheat: importance, sources of resistance, and heritability. In Proceedings, Fourth
722 International Wheat Genetics Symposium, Columbia, Missouri (pp. 465-470)
723 Rice, B., and A. E. Lipka, 2019 Evaluation of RR-BLUP genomic selection models that
724 incorporate peak genome-wide association study signals in maize and sorghum. Plant
725 Genome 12:180052 https://doi.org/10.3835/plantgenome2018.07.0052
726 Riedell, W. E., R. W. Kieckhefer, M. A. C. Langham, L. S. and Hesler, 2003 Root and Shoot
727 Responses to Bird Cherry-Oat Aphids and Barley yellow dwarf virus in Spring Wheat.
728 Crop Science, 43(4), 1380–1386 https://doi.org/10.2135/cropsci2003.1380

729 Rife, T. W., and J. A. Poland, 2014 Field Book: An Open-Source Application for Field Data
730 Collection on Android. Crop Science, 54(4), 1624–1627
731 https://doi.org/10.2135/cropsci2013.08.0579
732 Rouse, J. W., R. H. Haas, J. A. Schell, and D. W. Deering, 1974 Monitoring vegetation systems
733 in the Great Plains with ERTS. NASA special publication, 351(1974), 309
734 Rutkoski, J. E., J. A. Poland, R. P. Singh, J. Huerta-Espino, S. Bhavani, *et al*., 2014 Genomic
735 Selection for Quantitative Adult Plant Stem Rust Resistance in Wheat. The Plant
736 Genome, 7(3) https://doi.org/10.3835/plantgenome2014.02.0006
737 Sankaran, S., A. Mishra, R. Ehsani, and C. Davis, 2010 A review of advanced techniques for
738 detecting plant diseases. Computers and Electronics in Agriculture, 72(1), 1–13
739 https://doi.org/10.1016/j.compag.2010.02.007
740 Savary, S., L. Willocquet, S. J. Pethybridge, P. Esker, N. McRoberts, *et al*., 2019 The global
741 burden of pathogens and pests on major food crops. Nature ecology and evolution, 3(3),
742 430-439 https://doi.org/10.1038/s41559-018-0793-y
743 Shah, S. J. A., M. Bashir, and N. Manzoor, 2012 A review on barley yellow dwarf virus. In Crop
744 Production for Agricultural Improvement, Vol. 9789400741164, pp. 747–782
745 https://doi.org/10.1007/978-94-007-4116-4_29
746 Sharma, H., H. Ohm, L. Goulart, R. Lister, R. Appels, *et al*., 1995 Introgression and
747 characterization of barley yellow dwarf virus resistance from *Thinopyrum intermedium*
748 into wheat. Genome, 38(2), 406–413 https://doi.org/10.1139/g95-052
749 Singh, R. P., P.A. Burnett, M. Albarran, and S. Rajaram, 1993 *Bdv1*: a gene for tolerance to
750 barley yellow dwarf virus in bread wheats. Crop Science, 33(2), 231-234
751 https://doi.org/10.2135/cropsci1993.0011183X003300020002x
752 Singh, D., X. Wang, U. Kumar, L. Gao, M. Noor, *et al*., 2019 High-throughput phenotyping
753 enabled genetic dissection of crop lodging in wheat. Frontiers in plant science, 10, 394
754 https://doi.org/10.3389/fpls.2019.00394
755 Tola, J. E., and W. E. Kronstad, 1984The genetics of resistance to barley yellow dwarf virus in
756 wheat. In Barley Yellow Dwarf Workshop, Mexico, DF (Mexico), 6-8 Dec 1983.
757 CIMMYT

758 Walls, J., E. Rajotte, and C. Rosa, 2019 The past, present, and future of barley yellow dwarf
759 management. Agriculture (Switzerland), 9(1), 1–16
760 https://doi.org/10.3390/agriculture9010023
761 Wang, X., P. Silva, N. M. Bello, D. Singh, B. Evers, *et al*., 2020 Improved Accuracy of High-
762 Throughput Phenotyping from Unmanned Aerial Systems by Extracting Traits Directly
763 from Orthorectified Images. Frontiers in Plant Science, 11, 1616
764 https://doi.org/10.3389/fpls.2020.587093
765 Wang, X., D. Singh, S. Marla, G. Morris, and J. Poland, 2018 Field-based high-throughput
766 phenotyping of plant height in sorghum using different sensing technologies. Plant
767 Methods, 14(1), 53 https://doi.org/10.1186/s13007-018-0324-5
768 Zadoks, J. C., T. T. Chang, and C. F. Konzak, 1974 A decimal code for the growth stages of
769 cereals. Weed research 14.6 (1974): 415-421
770 Yin, LiLin, 2020 CMplot: Circle Manhattan Plot. R package version 3.6.2 https://CRAN.R-
771 project.org/package=CMplot
772 Yu, J., G. Pressoir, W. H. Briggs, I. V. Bi, M. Yamasaki, *et al*., 2006 A unified mixed-model
773 method for association mapping that accounts for multiple levels of relatedness. Nature
774 genetics, 38(2), 203-208 https://doi.org/10.1038/ng1702
775 Zhang, Z., Z. Lin, and Z. Xin, 2009 Research progress in BYDV resistance genes derived from
776 wheat and its wild relatives. Journal of Genetics and Genomics, 36(9), 567–573
777 https://doi.org/10.1016/S1673-8527(08)60148-4
778 Zheng, Q., W. Huang, X. Cui, Y. Dong, Y. Shi, *et al*., 2018 Identification of Wheat Yellow Rust
779 Using Optimal Three-Band Spectral Indices in Different Growth Stages. Sensors, 19(1),
780 35 https://doi.org/10.3390/s19010035
781

Table 1 – Field experimental details for the five wheat nurseries

Season	2015 – 2016	2016 – 2017	2017 – 2018	2018 – 2019	2019 – 2020
Location	Rocky Ford farm		Ashland Bottoms farm		
	39˚13'45.60" N, 96˚34'41.21" W		39˚07'53.76" N, 96˚37'05.20" W		
Planting Date	Sep. 17, 2015	Sep. 12, 2016	Sep. 19, 2017	Sep. 17, 2018	Sep. 17, 2019
Number of Entries	68	52	81	81	107
Number of Plots	504	360	400	392	684
Field Design	split-plot with insecticide treatment as major factor effect and wheat genotype as secondary factor				
Replications	3	3	2	2	2
Plot Size	6 rows plots - 1.5 m × 2.4 m				
BYD Evaluation	April 28, 2016	May 12, 2017	May 19, 2018	May 13, 2019	May 19, 2020
Harvesting Date	June 20, 2016	June 19, 2017	June 23, 2018	June 28, 2019	June 25, 2020

Table 2 – Dates of high-throughput phenotypic data collection and details of image acquisition in the five wheat nurseries screened for BYD, Kansas, USA (2015-2020).

Season	2015 – 2016	2016 – 2017	2017 – 2018	2018 – 2019	2019 – 2020
UAS Platform	PheMU		DJI Matrice 100		
Imaging Sensor	multiple digital single-lens reflex (DSLR) cameras		MicaSense RedEdge-M		
Flight/Pass speed	0.3–0.5 m/s		2 m/s		
Flight Dates	2016-03-31 2016-04-07 2016-04-14 2016-05-06	2017-03-28 2017-04-13 2017-05-01 2017-05-09 2017-05-21 2017-05-23 2017-05-30 2017-06-05 2017-06-13	2018-03-30 2018-04-04 2018-04-12 2018-04-19 2018-04-23 2018-05-16 2018-06-13	2019-04-01 2019-04-09 2019-04-19 2019-04-26 2019-05-02 2019-05-10 2019-05-15 2019-05-23 2019-05-31 2019-06-05 2019-06-12 2019-06-17	2020-03-20 2020-04-11 2020-04-23 2020-05-03 2020-05-19 2020-06-05 2020-06-11
Flight/Pass altitude	0.5 m above the canopy		20 m AGL		
In-Air Flight Duration	NA		~ 11–14 min		

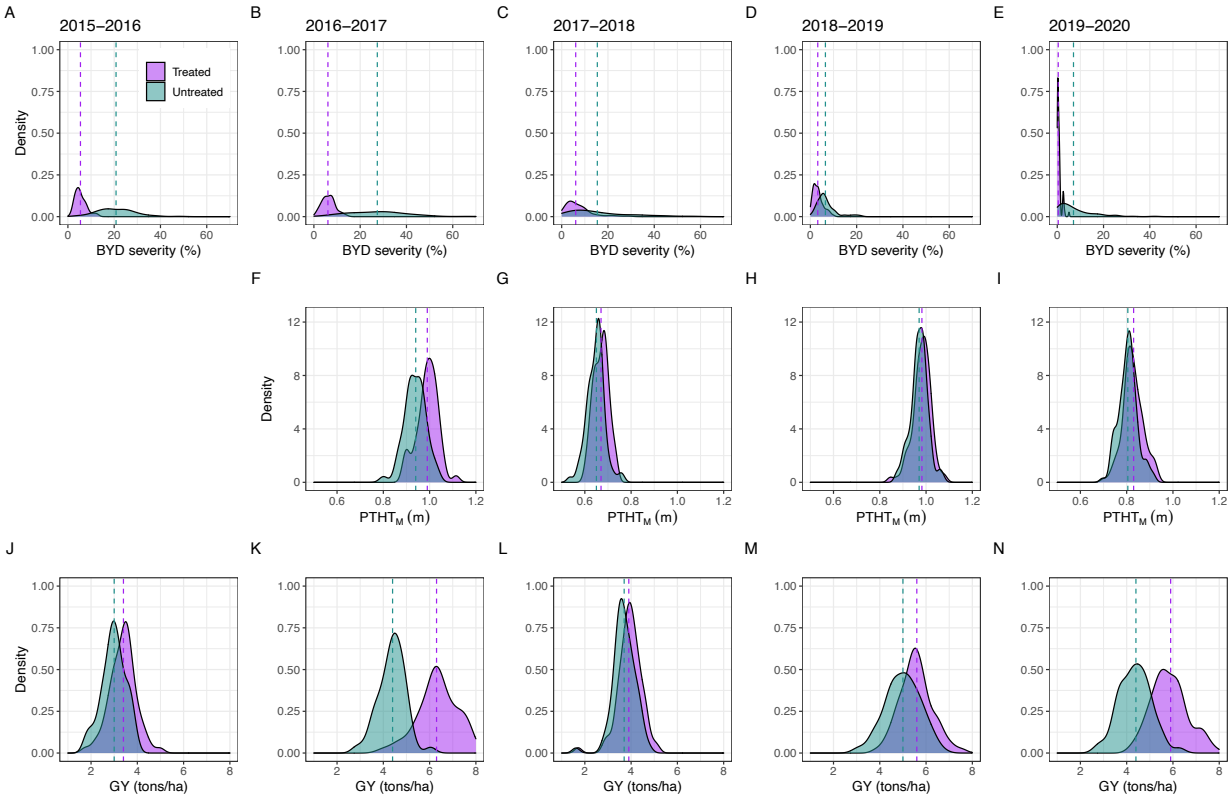

Figure 1 Adjusted phenotypic values for the traits collected manually for five different field seasons (2015-2016 to 2019-2020). A-E): barley yellow dwarf (BYD) severity (%) characterized as the typical visual symptoms of yellowing/purpling on leaves using a 0 – 100% visual scale, F-I) manual plant height/stunting ($PTHT_M$) (meters), note that the trait was not recorded for the 2015 – 2016 season, and J-N) grain yield (GY) (tons/ha). Insecticide-treated and untreated replications are represented by purple and green, respectively. The dashed line represents the mean value for the trait in each treatment

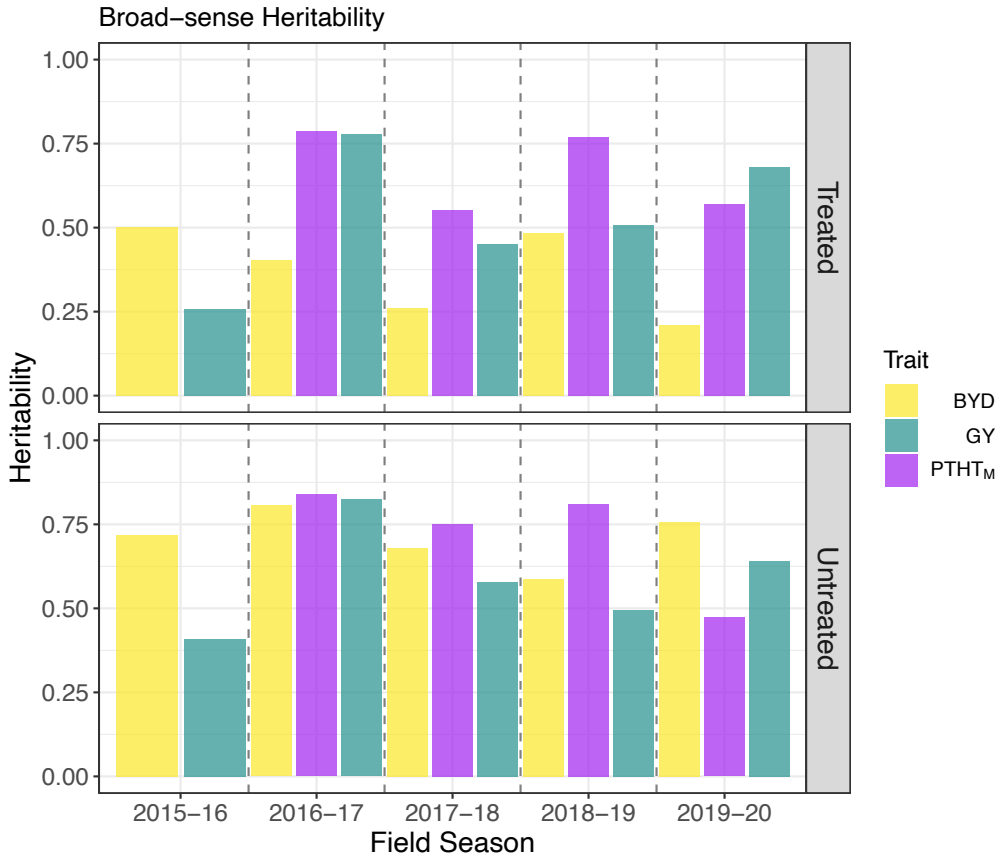

Figure 2 Broad-sense heritability of wheat phenotypic traits collected manually, including visual barley yellow dwarf (BYD) score, plant height ($PTHT_M$) and grain yield (GY) during five different field seasons under two insecticide treatments.

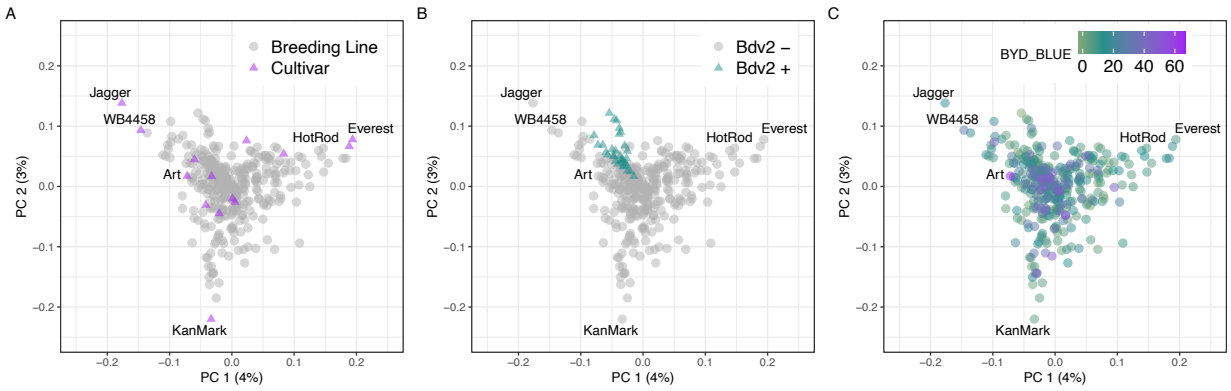

Figure 3 Scatterplot of the first two principal component axis, made from principal component analysis on the marker matrix, n = 357 wheat lines, markers = 29,480. Each data point represents an individual wheat line that is color-coded by A) breeding status, B) prediction of *Bdv2* presence/absence, and C) adjusted mean for BYD severity (BYD BLUE) scored visually. Total variance explained by each principal component (PC) is listed on the axis.

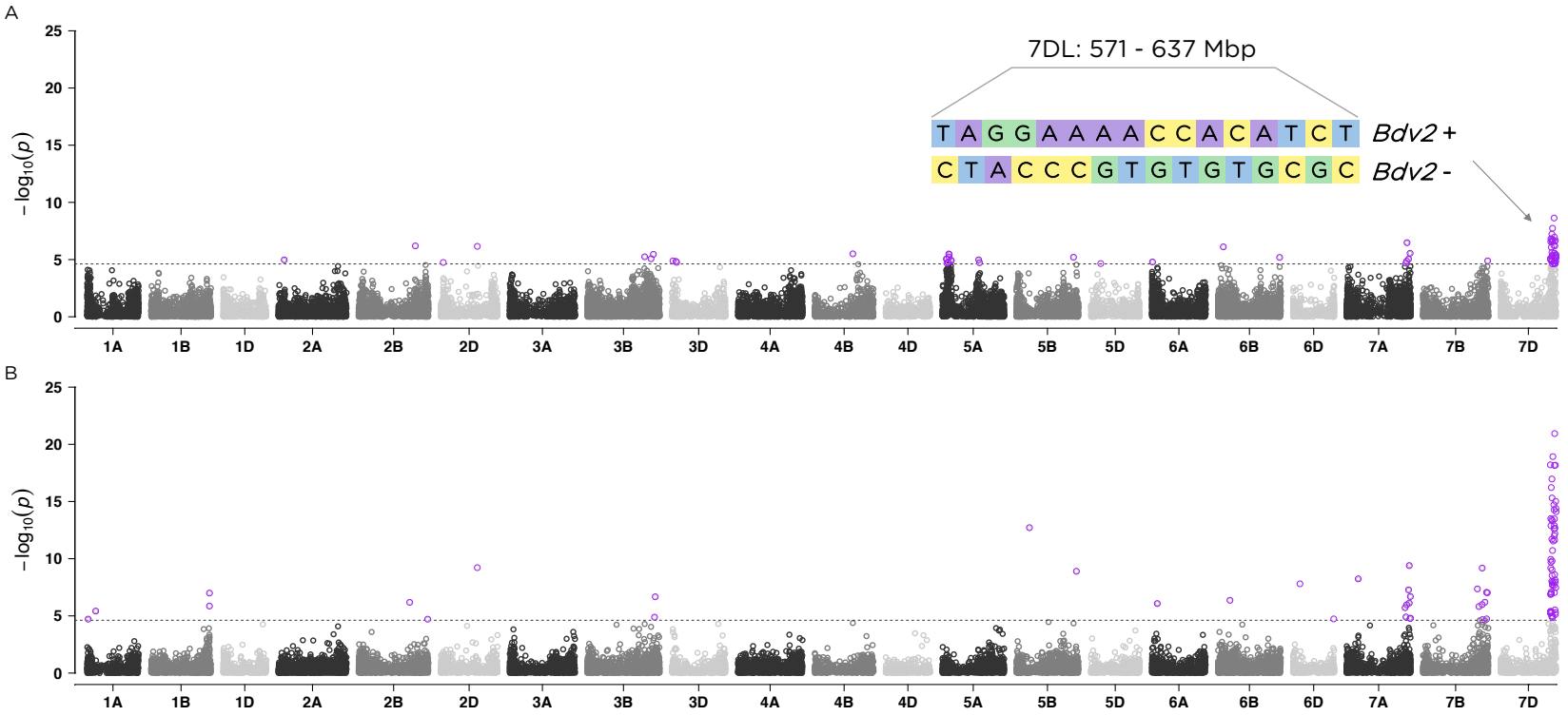

Figure 4 Manhattan plots showing the marker-trait associations using 346 wheat accessions and 29,480 SNP markers obtained with genotyping-by-sequencing (GBS) for A) BYD severity and B) presence/absence of *Bdv2* resistance gene. The 21 labeled wheat chromosomes with physical positions are on the x-axis and y-axis is the –log10 of the p-value for each SNP marker. Horizontal dashed lines represent the false discovery rate threshold at 0.01 level and data points highlighted in purple and above the threshold represent SNPs significantly associated with the trait. In panel a, the length of the region and the haplotypes defined by the significant SNP markers is displayed.

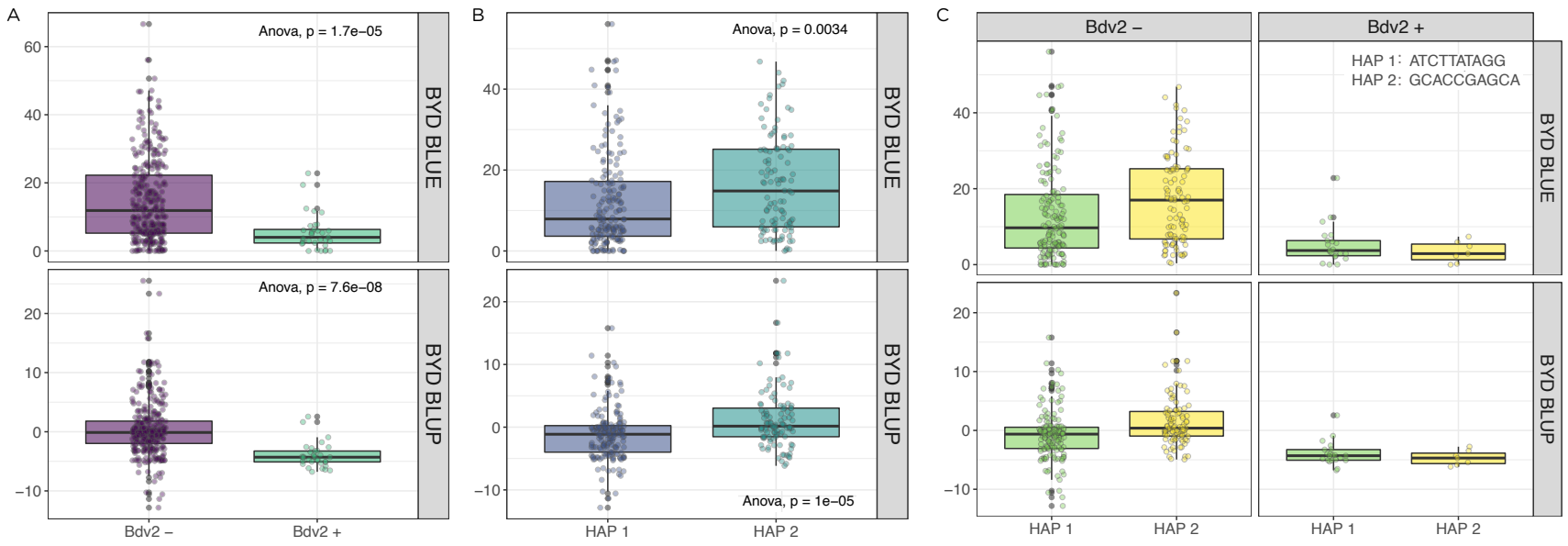

Figure 5 Measurement of barley yellow dwarf disease severity in wheat based on certain haplotype effects were panel A) represents the translocation segment carrying the resistance gene Bdv2, B) displays the two haplotypes for the significant region on chromosome 5AS, and C) shows the combination of Bdv2 resistance gene and 5A haplotype. Boxplots showing the significant reduction of BYD disease severity by averaging the phenotypic best linear unbiased estimated (BLUE) or best linear unbiased predicted (BLUP) values for the lines**.**

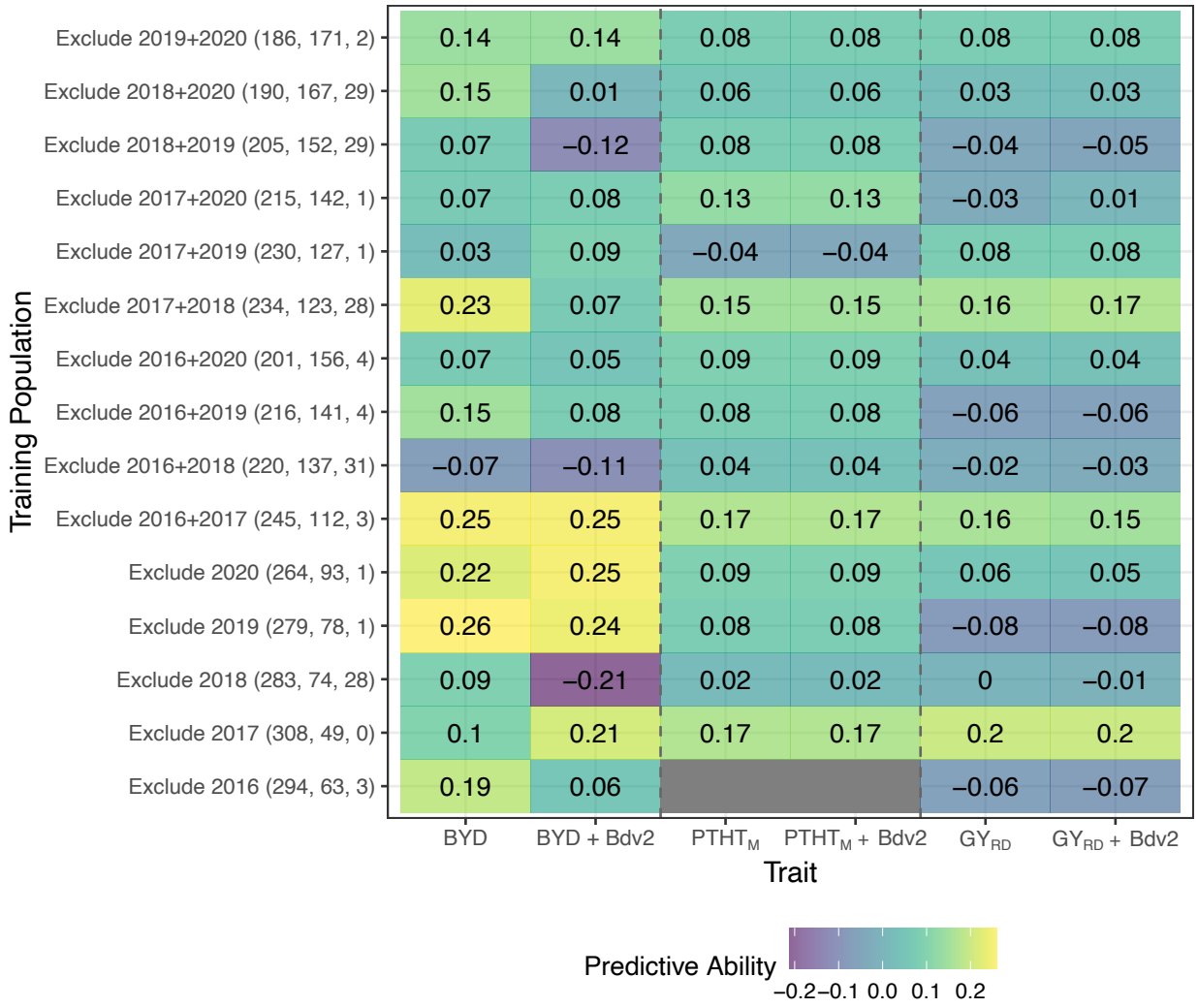

Figure 6 Genomic selection model predictive ability where each column represents one trait, and each row shows the conformation of the training population including size of training and testing population and number of lines with presence of *Bdv2* resistance gene. The value in each cell represents the predictive ability which is the correlation between the GS predicted value (GBLUP) and the phenotypic best linear unbiased predictor (BLUP).